Optical phase front control in a metallic grating with equally spaced alternately tapered slits*

Zheng Gai-Ge(郑改革)†, Wu Yi-Gen(吴义根), and Xu Lin-Hua(徐林华)

School of Physics and Optoelectronic Engineering, Nanjing University of Information Science & Technology, Nanjing 210044, *China*

(Received 10 December 2012; revised manuscript received 4 March 2013)

A technique capable of focusing and bending electromagnetic (EM) waves through plasmonic gratings with equally spaced alternately tapered slits has been introduced. Phase resonances are observed in the optical response of transmission gratings, and the EM wave passes through the tuning slits in the form of surface plasmon polaritons (SPPs) and obtains the required phase retardation to focus at the focal plane. The bending effect is achieved by constructing an asymmetric phase front which results from the tapered slits and gradient refractive index (GRIN) distribution of the dielectric material. Rigorous electromagnetic analysis by using the two-dimensional (2D) finite difference time domain (FDTD) method is employed to verify our proposed designs. When the EM waves are incident at an angle on the optical axis, the beam splitting effect can also be achieved. These index-modulated slits are demonstrated to have unique advantages in beam manipulation compared with the width-modulated ones. In combination with previous studies, it is expected that our results could lead to the realization of optimum designs for plasmonic nanolenses.

Keywords: surface plasmon polaritons, optical phase front control, metallic grating, nanophotonic device

PACS: 42.79.Fm, 42.25.–p, 42.79.Ry **DOI:** 10.1088/1674-1056/22/10/104212

1. Introduction

Recent investigations of guided surface plasmon wave (GSPW) devices have focused on their abilities to propagate light in channels of diameters significantly below the dielectric diffraction limit, and shown that they have promise to become highly integrated opto-electronical devices.[1–5] One of the possible applications is a plasmonic lens based on nanometallic slits that function as refractive dielectric optical elements in beam shaping and can achieve subwavelength scale focal zones.[6–18] They have proven to be useful in numerous areas such as nanofabrication, nanophotonic circuits, circular polarizer analyzers, etc.[9–11,13,14]

There are usually two kinds of strategies for manipulating beams or focusing light in the air with surface plasmon polaritons (SPPs), the first one is to use a sub-wavelength metal slit surrounded by surface gratings,[17–19] and the second one is to adopt multiple metallic waveguides.[20–22] The first method to generate beams is to make SPPs, which are excited on corrugated metal surface from a sub-wavelength metal slit, radiate into a certain direction by using surface gratings. Because the radiation direction of an SPP depends on the profile of the surface grating, one can render beams by adjusting the surface grating profile.[20,21] The second method to manipulate beams is to control the phase of the SPP induced in a metallic waveguide, which ends up with it radiating at the output surface of the metallic waveguide.[6–8] If it is possible to control the phase of SPPs radiating at the output surface, one can manipulate beams based on Huygens' principle.

Recently, phase resonances have been observed in the microwave response of metal transmission gratings comprised of identical but alternately orientated tapered slits.[23] The excitations of high-Q modes are attributed to the interference between Fabry–Pérot (FP)-like modes and diffractively coupled surface waves. Tapered structures have been proven to be very useful in the design of plasmonic waveguides because of surface plasmon mode confinement and enhanced transmission through the aperture.

In this paper, we extend the previous studies and examine the ways of controlling the phase front of the transmitted beam by using a metallic grating with equally spaced alternately tapered slits. Before discussing the focusing effect, extraordinary optical transmission (EOT) in periodic arrays of tapered slits instead of straight slits is considered. The numerical results show that the tapered grating leads to a dramatic enhancement of the transmission over a broadband wavelength range and the focusing behavior can be adjusted by changing the orientation of alternate tapered slits. In addition, the beam deflection angle of the transmitted beam will be changed as the refractive index configuration of the metallic grating varies.

2. Theoretical analysis and structure

The representation of the proposed transmission grating with a thickness of h is shown in Fig. 1. The grating is laid on the xy plane, the slit interspacing from center to center is Λ. A

*Project supported by the National Natural Science Foundation of China (Grant Nos. 61203211 and 20907021) and the Foundation for Outstanding Young Teachers of Nanjing University of Information Science & Technology, China (Grant No. 20110423).

†Corresponding author. E-mail: eriot@126.com

© 2013 Chinese Physical Society and IOP Publishing Ltd

TM-polarized plane wave normally illuminates the slit array from the left side. Γ and Γ' represent the structure exit plane and the observation plane where the light should be focused, respectively. The f represents a focal length of the designed lens which is equal to the distance between the exit plane Γ and the observation plane Γ'. The wave function on the exit plane is denoted as H_{1z} and the wave function on the observation plane is represented with H_{2z}.

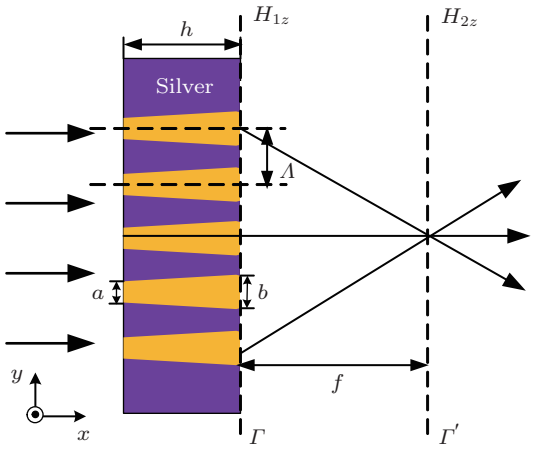


Fig. 1. (color online) Schematic diagram of a grating formed on a thin metallic film, where metal thickness h and the slit interspacing Λ (center to center) are equal. A transverse magnetic (TM) plane wave is incident onto the SPP lens from the left side.

The gap distance between two adjacent nanoslits should be larger than the metal skin depth to prevent the coupling of SPPs in the propagation process. Thus the complex amplitude distribution ($H_{1z}(\Gamma)$) on the exit plane of structure can be expressed as the sum of amplitude and phase distribution of each slit. The amplitude and phase distribution at the exit port of each slit is calculated by using the FDTD method.

On reaching the exit of the slit, the SPP mode will be decoupled into a radiative mode which radiates in all directions, as a point source does in half-space.[6] Therefore we can model the nano-slits as point sources which are located at the exit of slits. Then, the field in the observation plane can be obtained by the linear superposition of waves originating from each slit using[24]

$$H_{2z}(\Gamma') = \sum_n \frac{H_{1z}(\Gamma)}{\sqrt{r}} \exp(\mathrm{i}k_0 r), \tag{1}$$

where $r = \sqrt{f^2 + (\Gamma_n - \Gamma'_m)^2}$, Γ_n and Γ'_m being the positions of slits and the observation points, respectively.

Zhao *et al.*[15] illustrated that the phase difference caused by distances between slits will not play a dominant role in the design of an asymmetric plasmonic lens. Thus in our work, we construct asymmetric phase front profiles by modulating the geometric parameters of slits and the index distributions, rather than adjusting inter-slit spacing.

3. Simulation results and discussion

The FDTD method is used to study the transmission properties of this metallic grating structure with the perfectly matched layer (PML) absorbing boundary conditions in x and y directions of the simulation domain. In the following FDTD simulations, the grid sizes in the x and y directions are chosen to be $\Delta x = \Delta y = 2$ nm and $\Delta t = \Delta x/2c$, which are sufficient for the numerical convergence, where c is the velocity of light in vacuum. The metal is chosen to be silver (Ag) in this paper and the frequency-dependent relative permittivity can be characterized by the Drude model:

$$\varepsilon_m(\omega) = \varepsilon_\infty - \frac{\omega_\mathrm{p}^2}{\omega^2 + \mathrm{j}\gamma_\mathrm{p}\omega}, \tag{2}$$

where ε_∞ is the dielectric constant at infinite angular frequency, ω_p and γ_p are the plasma and collision angular frequency, respectively. All the parameters of the Drude model can be found in Ref. [25].

3.1. EOT and focusing effect of the grating with tapered slits

The research on plasmonics has been burgeoning with the discoveries of EOT through periodic sub-wavelength metal slits and beaming from a sub-wavelength metal hole surrounded by groove or gratings. The EOT offers large transmission and localized field enhancements, with potential applications in areas such as optical displays, near-field microscopy, sensing and bio-photonics. Most of the previous work concentrated on the transmittance of metallic gratings with straight narrow slits.[5–8,15–19,26,27] Both cavity mode and SP excitation contribute to the extraordinary transmission for slit arrays. Before discussing the focusing effect of our proposal, we will consider the EOT in periodic arrays of tapered slits instead of straight slits. The initial parameters are as follows: $h = 800$ nm, $\Lambda = 500$ nm, $b = 100$ nm, the entrance aperture size a is tuned.

Figure 2 shows the calculated TM transmissions with normal incidence. FP resonance peaks can be observed for gratings with straight sidewalls. For various parameters, the tapered grating leads to a dramatic enhancement of the transmission over a broadband wavelength range, comparing the straight sidewall case with the tapered cases, though the peak transmission becomes smaller by tapering. In addition, we notice that with increasing a, the transmission resonance wavelength presents a blue shifting at fixed film thickness which can be explained from the FP resonance condition as follows:[28]

$$2\int_0^h \beta_\mathrm{GSP}(x)\,\mathrm{d}x + \varphi_\mathrm{R} = 2\pi m, \tag{3}$$

where β_GSP is the propagation constant of an SPP wave in an air gap between two closely spaced gold surfaces, x is the position along the center of the slit, φ_R is the total reflection

phase per round-trip associated with reflection of the gap surface plasmon polariton (GSPP) wave at the termination of the slit, and m is an arbitrary integer. The propagation constant of a GSPP is very sensitive to the width of the slit and decreases with slit width increasing, while it increases with wavelength decreasing.[9,17] Thus as the entrance aperture size increases the free-space resonance wavelength must decrease according to Eq. (3) if we keep the film thickness h fixed.

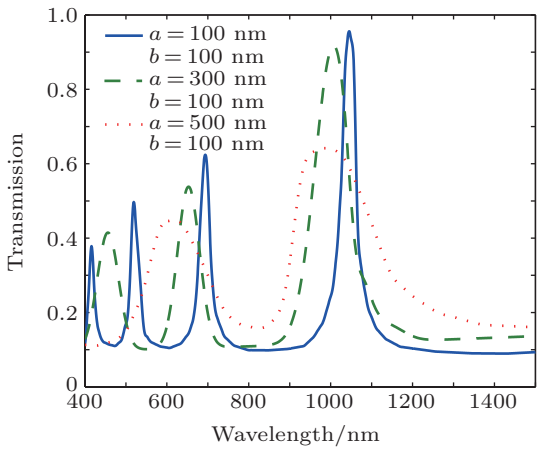


Fig. 2. (color online) Transmissions for a tapered slit array with different sizes from numerical simulation by FDTD method.

When TM polarized waves impinge on the entrance surface of a silver slab, SPPs are excited.[29] In the tapered slit, the incident light is converted into gap surface plasmon polaritons (GSPPs), which propagate adiabatically through the slit.[30] At the exit aperture of the tapered slit, the GSPPs in the tapered slit will be converted into SPPs, because SPPs can only propagate along the air/metal interface. The radiating fields at the ends of metallic slits each can be regarded as an individual point source. While wave propagation is in the shape of the spherical wave from the sources into the air, they are focused at the specific point due to the constructive interference. We first consider a planar structure containing five slits. The paramaters are chosen as $a = b = 100$ nm, $\Lambda = 500$ nm, and $h = 800$ nm. In order to show the performance of the designed structure, the structure is checked by the FDTD method and the intensity distribution of $|H_z|$ is demonstrated in Fig. 3(a). One can see clearly the light focusing. The focal point is defined as the point where transmitted intensity reaches the maximum. The focal length, denoted by f in the following, is the distance from the exit of the array to the focal point. Under normally incident radiation with a wavelength of 633 nm, a clear focal spot appears at 2.4 μm away from the exit plane Γ, which agrees with our preassigned position well. The cross section at focal spot in the y direction is given in Fig. 3(b), indicating an FWHM of 1 μm which is larger than the incident wavelength. To realize the subwavelength focusing effect, the genetic algorithm (GA) and the Yang–Gu (YG) algorithm can be obtained to optimize the structural parameters which are width, length, and gap of the metallic slits.[31,32]

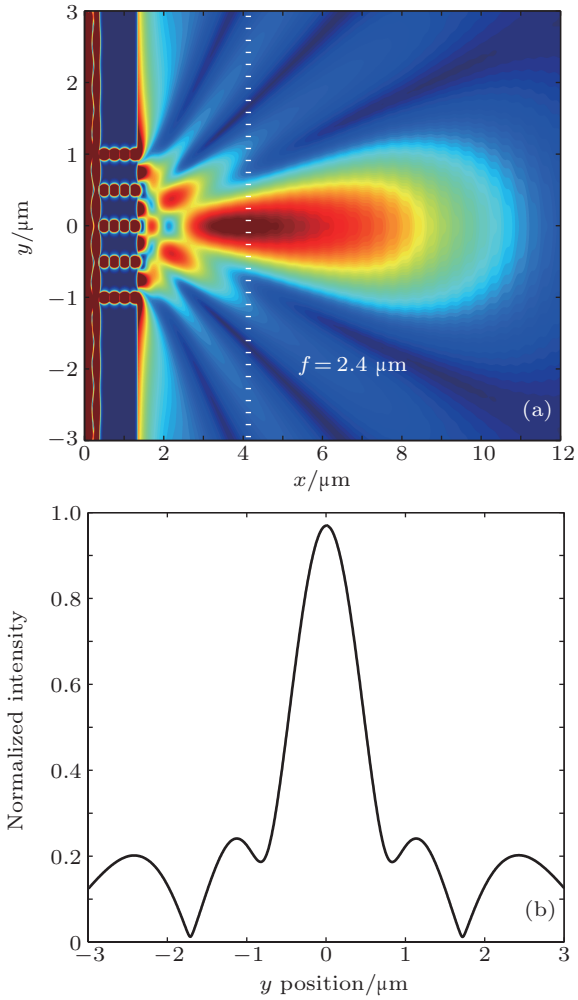


Fig. 3. (color online) (a) Intensity distribution of the designed nanodevice, calculated using the FDTD method when the incident wavelength is 633 nm. The structure's exit plane is positioned at 1350 nm. (b) Cross section of the focal spot.

Assuming that the width of each nanoslit is much smaller than the incident wavelength, it is reasonable just to consider the fundamental mode in the nanoslit. An analytical expression for the effective index of the fundamental TM_0 mode (coupled SPP approximation) can be obtained as[33]

$$n_{\text{eff}} = \sqrt{\varepsilon_{\text{d}}}\left(1+\frac{\lambda}{\pi w}\sqrt{1-\frac{\varepsilon_{\text{d}}}{\varepsilon_{\text{m}}}}\right)^{1/2}, \tag{4}$$

where w is the aperture of the waveguide, λ is the wavelength of incident optical wave, ε_{d} and ε_{m} represent the permittivities of the dielectric medium in the slit and the metal, respectively. In the case of a tapered waveguide, the slit width w varies with propagation distance, and the effective index varies accordingly. Nevertheless, we can use the above equation to analyze the effective refractive index (ERI) of the tapered plamonic waveguide.

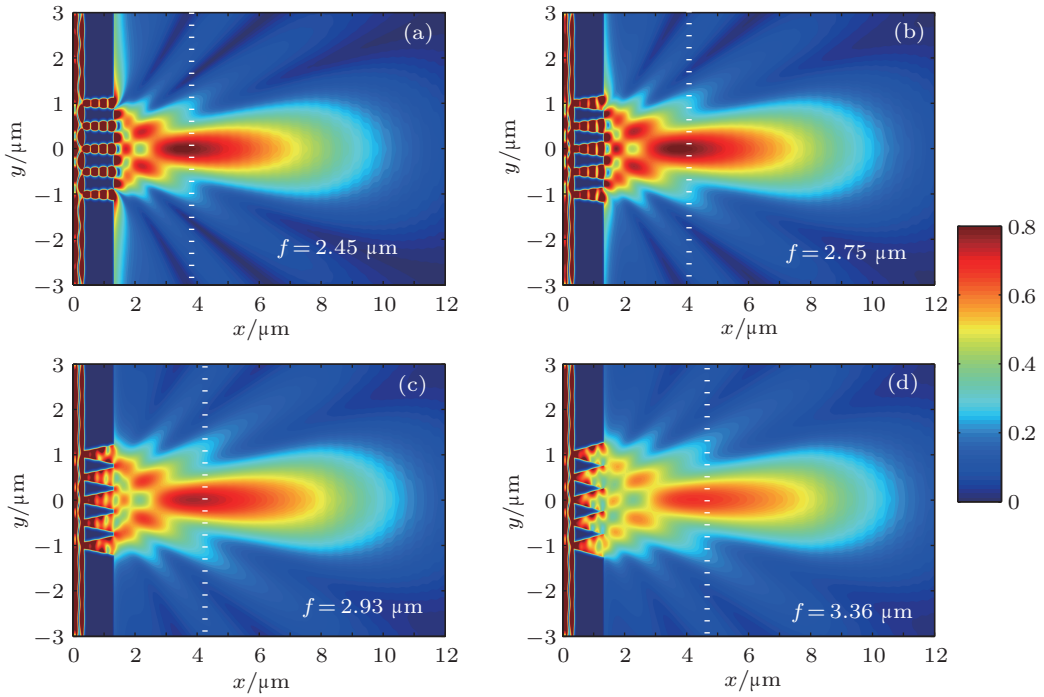


Fig. 4. (color online) Intensity distributions of the designed plamonic lens, calculated using the FDTD method. The slit length h, spacing Λ, and input aperture a are kept constant, $h = 1000$ nm, $\Lambda = 500$ nm, $a = 100$ nm, the output aperture b is the only variable. (a) $b = 200$ nm; (b) $b = 300$ nm; (c) $b = 400$ nm; (d) $b = 500$ nm.

In the following design, we first keep the slit length h, spacing Λ, and input aperture a constant, the output aperture b is the only variable. We observe that the focal lentgh is proportional to output aperture (b). As shown in Figs. 4(a)–4(d), as b increases from 200 nm to 500 nm, the focal length (f) increases from 2.45 μm to 3.36 μm. This phenomenon results from the decrease of the ERI when the output aperture increases.

As discussed in the previous section, the field at the observation plane can be obtained by linear superposition of waves originating from each slit. The field intensity at the structure's exit plane reduces with output aperture increasing as verified by FDTD calculation. Thus the field intensity in the observation plane also reduces with output aperture increasing.

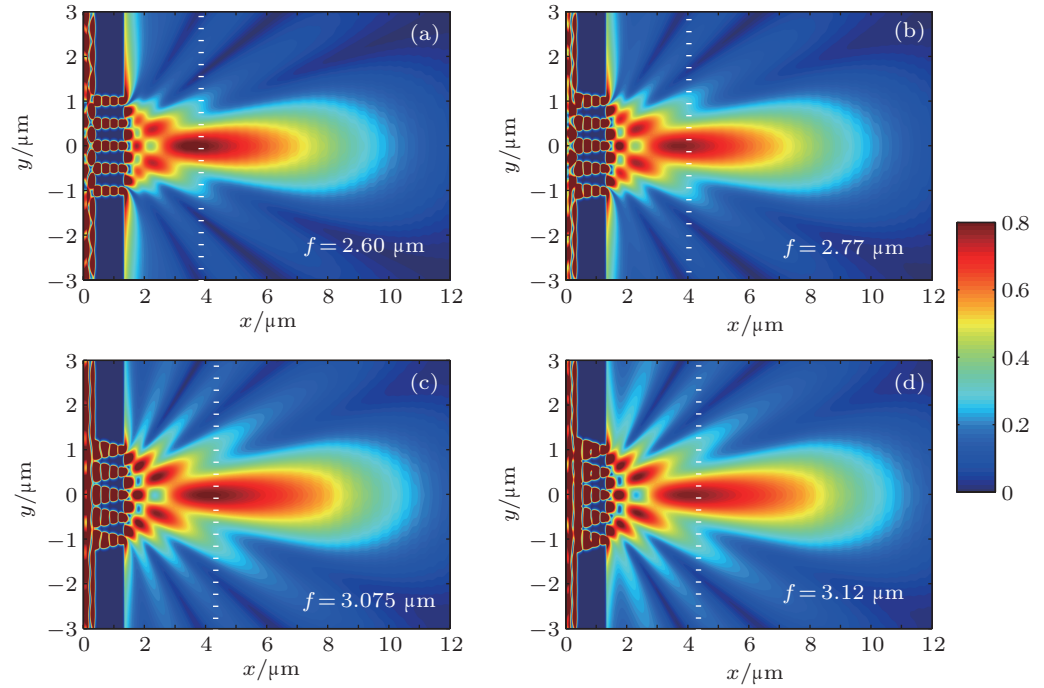


Fig. 5. (color online) Intensity distributions of the designed plamonic lens calculated using the FDTD method. The slit length h, spacing Λ, and output aperture b were kept as constant, $h = 1000$ nm, $\Lambda = 500$ nm, $b = 100$ nm, the input aperture a is the only variable. (a) $a = 200$ nm; (b) $a = 300$ nm; (c) $a = 400$ nm; (d) $a = 500$ nm.

In the second step, we keep the slit length h, spacing Λ, and output aperture b constant, the input aperture a is the only variable. The main advantage of a tapered waveguide over a rectangular one lies in its superior surface plasmon mode confinement.[15] The second advantage of using tapered structures is that the enhanced transmission can be obtained when the input aperture is larger than the output aperture.[34] Figures 5(a)–5(d) further illustrate the corresponding H-field intensity distributions for four different values of a. The H-field intensity distributions show that the energy emerging from the structure tends to focus within several micrometers in an extremely small region. When a increases to certain value, f almost keeps constant. This is because the complex transmission coefficient (β) gradually decreases as the slit width increases. If the slit width goes to infinity, the transmission coefficient approaches unity in the air. When a is larger than 100 nm, the complex transmission coefficient changes very slowly which results in the small change of f.

Under adiabatic approximation, the plasmon wave vector and its location and field distribution are determined at each distance from the tip of tapered waveguide. The dispersion relation for the plasmon in the taper SPP structure is given approximately as [35,36]

$$\frac{\varepsilon_{\rm d}}{\varepsilon_{\rm m}} = -\frac{h_{\rm d}}{h_{\rm m}} \frac{{\rm K}_0(h_{\rm d}r){\rm I}_1(h_{\rm m}r)}{{\rm K}_0(h_{\rm d}r){\rm I}_0(h_{\rm m}r)}, \tag{5}$$

where $h_{\rm d} = \sqrt{q^2 - k_0^2\varepsilon_{\rm d}}$ and $h_{\rm m} = \sqrt{q^2 - k_0^2\varepsilon_{\rm m}k_0}$ being the wave number in the free space; ${\rm I}_p$ and ${\rm K}_p$ $(p = 0, 1)$ are the modified Bessel functions; r is the local diameter of the waveguide. The real and imaginary parts of β determine the phase velocity and propagation loss, respectively. In Fig. 6, the complex transmission coefficient β normalized by free space wave number k_0 as a function of slit width is plotted with the solid line. It is seen that the complex wave number gradually decreases as the slit width increases. If the slit width goes to infinity, the solid line approaches the dotted line which denotes the wave number in the air.

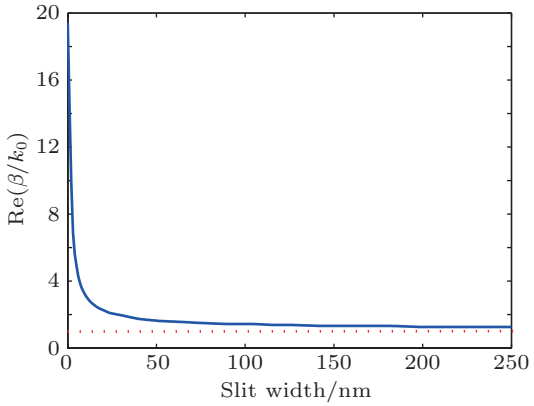


Fig. 6. (color online) Complex transmission coefficient β of the SPP as a function of input aperture (a). Output aperture (b) is fixed at 100 nm here. The upper and lower lines denote the SPP mode in the metallic slit and the transmission coefficient of the light line in air, respectively.

Fundamentally, the focusing effect of the stack array can be ascribed to the multiple interferences of SP waves from each tapered slit. In our design, we just use five slits to realize beam focusing. The main difference between the structure having a few slits and the structure with infinite slits is that the latter can efficiently couple the incident light into SP antisymmetric modes through momentum matching by diffraction, and therefore the efficiency would be much higher.[37] Our analysis and calculated results indicate that very compact structures with just a few slits can still perform the beam focusing function.

The methods to manipulate beam by modulating light phase through a metallic film with arrayed nano-slits which have constant depth but variant widths have been proposed.[7,16,38] The slits transport electro–magnetic energy in the form of SPPs and provide desired phase retardations of beam manipulating with variant phase propagation constant. In our design, because of the equal widths, depths, and interspaces between the metal slits, there would be no focusing effect for infinite waveguide array. However, we have observed a focal spot in the designed tapered structure and we suppose that the finite-size effect is important in this process. To further explore the focusing effect of the designed structures, we analyze the FDTD calculated phase distribution as shown in Fig. 7. The position of the focal spot can easily be identified as the curved wavefront and phase converging point when the structrue contains five slits (Figs. 7(a) and 7(c)). As the number of slits increases, we cannot see any focal spots (Figs. 7(b) and 7(d)). According to previous studies,[7–9,15,16] the lens parameters are greatly affected by the lens size and larger lens size (more slits are used) will produce a better focusing behavior. Our results show different phenomena as a result of the usage of tapered waveguide array.

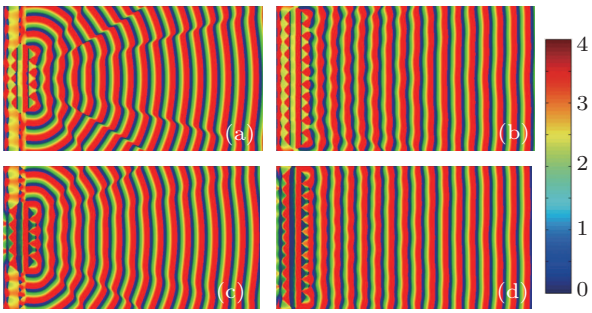


Fig. 7. (color online) FDTD calculated phase distributions for the designed structures. (a) $a = b = 100$ nm with five slits; (b) $a = b = 100$ nm with eleven slits; (c) $a = 300$ nm, $b = 100$ nm with five slits; (d) $a = 300$ nm, $b = 100$ nm with eleven slits. The other parameters are the same as those in Fig. 3.

3.2. Beam bending with the changing of refractive index distribution

The positional and directional modulation functionalities of a plasmonic lens are determined by the relative phase difference between neighboring slits. The authors in Ref. [15] created a relative phase difference profile across the width of

the lens by introducing a continuous change to the slit geometry along the transverse direction. An asymmetric phase front across the plasmonic lens has been bulit to achieve directional modulation. The slits may be filled with an index-tunable medium and the plasmonic grating will act like an optical phased array. As in a uniform linear array of equally spaced antennas, the relation between output steering angle θ and phase difference $\Delta\varphi$ between adjacent slits is given by

$$\Delta\varphi = \frac{2\pi}{\lambda}\Lambda \sin\theta,$$

where Λ ($\Lambda = a+b$) is the pitch and λ is the wavelength of the input beam. This relation suggests that a larger bending angle needs a larger phase difference between adjacent slits.

When the SPP mode passes through the sub-wavelength metallic slit, output phase $\Delta\varphi$, the phase retardation of the transmitted light, is expressed as[38]

$$\Delta\varphi = \mathrm{Re}(\beta h) + \arg\left[1 - \left(\frac{1-\beta/k_0}{1+\beta/k_0}\right)^2 \exp(2\mathrm{j}\beta h)\right], \quad (6)$$

where h is the length of the metallic slit. The first term, phase retardation βh, comes from SPP propagation in the metallic slit. The second term is the phase retardation which results from multiple reflections between the entrance and end of the metallic slit. Both physical analysis and numerical simulations show that the phase retardation is dominantly determined by the real part of β. Therefore, $\Delta\varphi$ can be approximated as $\mathrm{Re}(\beta h)$, and it could be obtained from Eqs. (4) and (5) that the phase retardation can be tuned by changing the refractive index in the slit when other parameters are fixed. When the materials filled in the two adjacent slits are different, the phase retardations of light transmitted are also different, the phase difference between adjacent slits is determined by $\Delta\varphi_{n,n+1} = \mathrm{Re}(\beta_{n+1}h) - \mathrm{Re}(\beta_n h)$. The steering angle can be controlled by changing the index distribution.

The simulated structure consists of 6 silver (Ag) layers that alternate with 5 dielectric layers, and it is plotted schematically in Fig. 8. The relative permittivity of the dielectric layer is expressed as

$$\varepsilon_n = \varepsilon_1 + (n-1)\alpha, \quad (7)$$

where n is the ordinal number of each dielectric layer, ε_1 is the relative permittivity of the first dielectric layer, and α is the gradient of the relative permittivity. Such a gradient can be achieved by cosputtering two different oxide sputtering targets with precisely adjusting the electrical power for the two targets.[39]

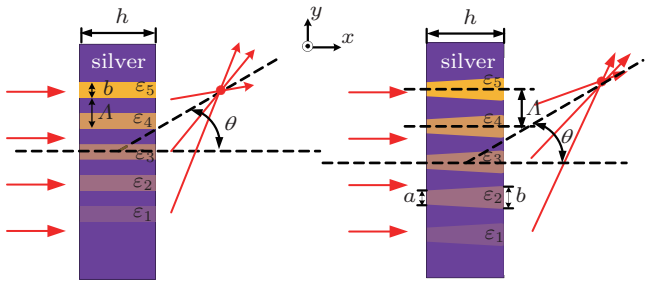


Fig. 8. (color online) Schematic plot of the proposed structure that can bend a light beam or focal point in transverse direction. A TM wave is incident from the left side of the structure. (a) Grating with a planar MDM slit array; (b) Grating with equally spaced alternately tapered slits.

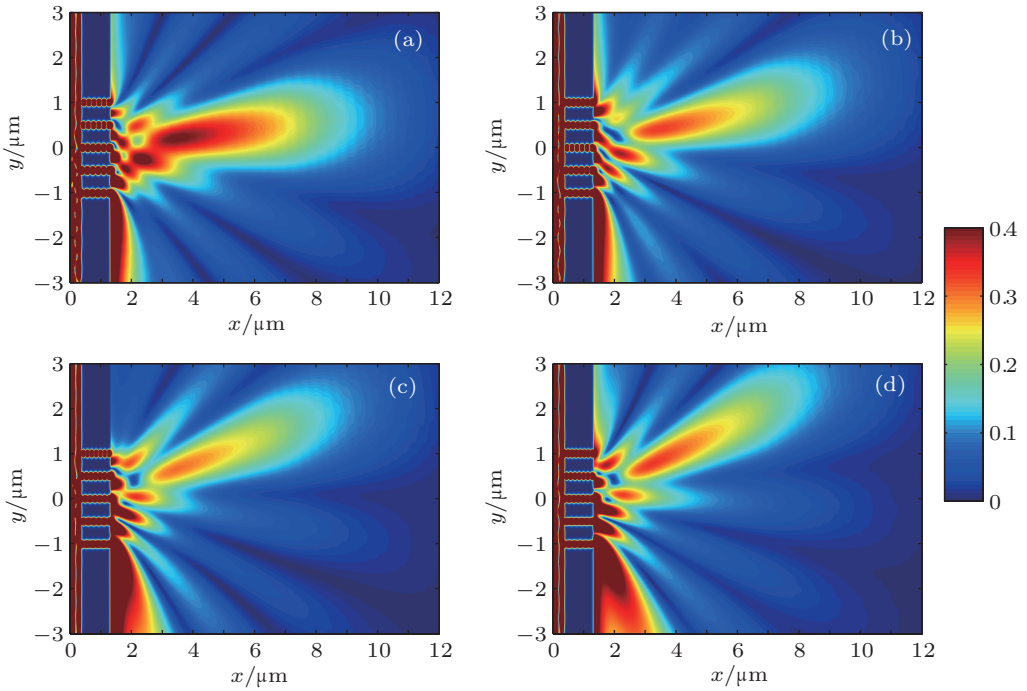


Fig. 9. (color online) H-field intensity profiles of the proposed structure with different refractive index distributions of the dielectric material in a grating with planar slits. (a) α=0.1; (b) $\alpha = 0.2$; (c) $\alpha = 0.3$; (d) $\alpha = 0.4$. The results show that the plane waves can propagate with 8.2°, 14.6°, 28.3°, and 42° beam deflections, respectively, after propagating through the proposed planar grating.

Figures 9(a)–9(d) plot the simulated contours of the magnetic field intensities for $\alpha = 0.1$, 0.2, 0.3, and 0.4, respectively, when $\varepsilon_1 = 2$. Under normally incident radiation with a wavelength of 633 nm, beam deflections with 8.2°, 14.6°, 28.3°, and 42° can be observed from the simulation due to the constructive interference among the phase-delayed, transmitted waves from the rectangular slits of the proposed planar grating. The asymmetric phase front causes the light beam to bend off the central axis.

Based on the effective medium approximation theory, the proposed structure can be considered as an effective medium with a graded effective dielectric permittivity. By varying the refractive indices of the dielectric layers, the effective permittivity of the whole structure is changed at the same time. If the refractive index distribution for the beam-steering device has the following form:[40,41]

$$n(y) = n_0 + \frac{\sin\theta}{h} y,$$

where n_0 is the refractive index along the y axis, the beam deflection can be realized. The key point for beam deflection from a plasmonic device involves careful optimizations of the width and position of each slit for the desirable phase retardation.[42] In our design, the deflection angle of the transmitted beam can be controlled by varying the refractive index configuration of the nanoslit array.

We can employ tapered slits to form an asymmetric phase front for beam bending that has been proven to be useful in the design of plasmonic waveguides.[41] As can be seen from plots presented in Fig. 10, the interference pattern of the transmitted light exhibits a focal spot with a deflection angle. The bending angles can be controlled not only by the asymmetric phase front caused by continuously varying tapered slits when EM waves pass through the plasmonic lens but also by the index distributions.

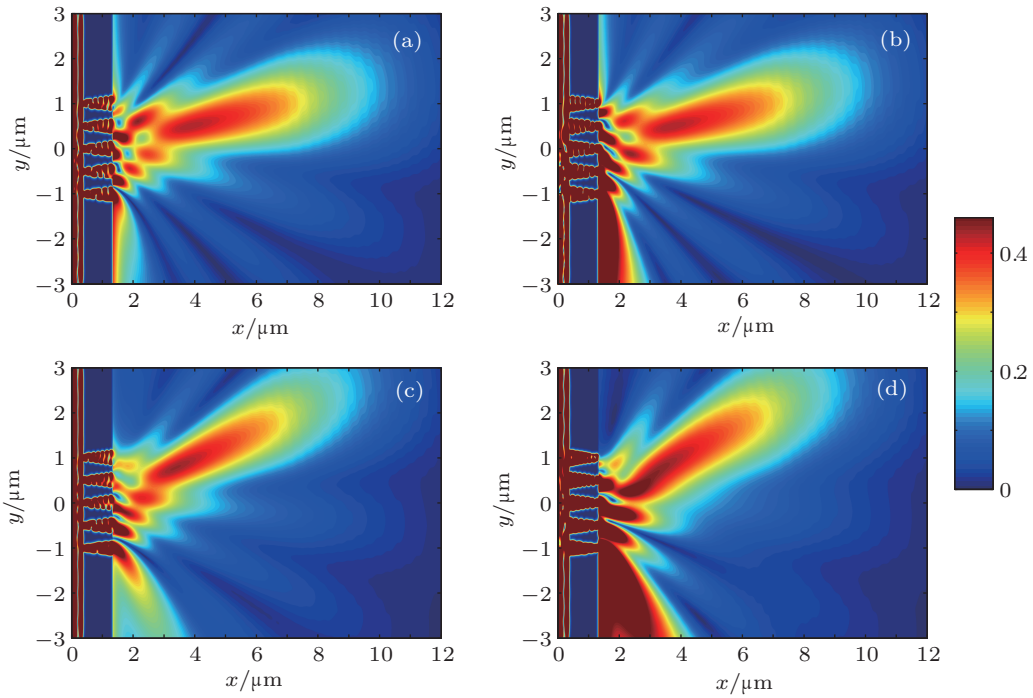


Fig. 10. (color online) H-field intensity profiles of the proposed structure with different refractive index distributions of the dielectric material in a grating with tapered slits. (a) $\alpha = 0.2$, $a = 100$ nm, $b = 300$ nm; (b) $\alpha = 0.2$, $a = 300$ nm, $b = 100$ nm; (c) $\alpha = 0.4$, $a = 100$ nm, $b = 300$ nm; (d) $\alpha = 0.4$, $a = 300$ nm, $b = 100$ nm.

In the above considerations, the incident light is normal to the grating surface. We proceed to investigate the compound grating performance when the EM waves are incident at an angle with respect to the optical axis. In Figs. 11(a) and 11(b), light impinges on gratings at angles of 20° and 40° with respect to the optical axis, respectively. Such a condition adds an extra planar phase front that interferes with the asymmetric phase front of the plasmonic lens, leading to a larger bending angle off the axial direction. From the magnetic field distribution in Fig. 11, one can see that the beam splitting effect can be achieved by changing the incident angle. The nanoslits with different widths and depths can lead to different phase retardations while the surface plasmons passing through the structure. Thus beam splitter and deflector can be realized by adjusting the widths and depths of the slits accordingly.[42–44] In our design, because of the gradient index distribution of the dielectric material in the grating, the asymmetric phase front will result in a beam splitting phenomenon which is different from previous proposals.

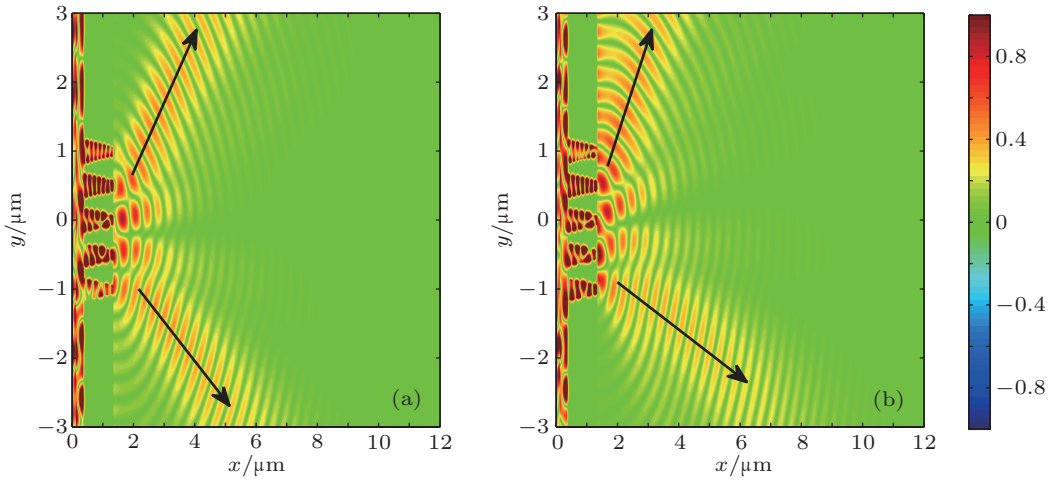


Fig. 11. (color online) Magnetic field distributions of the designed plamonic beam splitter. (a) $\alpha = 0.2$, $a = 300$ nm, $b = 100$ nm; (b) $\alpha = 0.4$, $a = 300$ nm, $b = 100$ nm.

4. Conclusion

In this paper, we study the EM response of gratings with equally spaced alternately tapered slits, and introduce a design principle for plasmonic lenses that can bend light along the direction transverse to the propagation direction. Not only the tapered slits but also the refractive-index distributions contribute to the focusing and bending effect. Light bending is achieved by constructing a carefully designed, curved phase front for the plasmonic lens. The control of the phase front profile is achieved through two mechanisms: phase retardation caused by the width and shape of the individual slit, and the refractive-index distributions in the grating. Furthermore, it is confirmed that the beam splitting effect can be achieved by changing the incident angle. Such a dynamical control of the beam direction can lead to other applications of nanolenses. This may constitute a new basis for potential applications in photonic and plasmonic devices and open up a new avenue to achieve the optimal design of diffractive optical elements on the subwavelength scale.

Acknowledgments

The authors would especially like to thank Prof. Xiao Shao-Rong and Dr. Su Wei from NUST for their useful discussions.

References

[1] Zia R, Schuller J A, Chandran A and Brongersma M L 2006 *Mater. Today* **9** 20
[2] Dionne J A, Sweatlock L A, Atwater H A and Polman A 2006 *Phys. Rev. B* **73** 035407
[3] Zhong R B, Liu W H, Zhou J and Liu S G 2012 *Chin. Phys. B* **21** 117303
[4] Zhu Y J, Huang X G and Mei X 2012 *Chin. Phys. Lett.* **29** 064214
[5] Wang C, Chen J J, Tang W H and Xiao J H 2012 *Chin. Phys. Lett.* **29** 127304
[6] Sun Z J and Kim H 2004 *Appl. Phys. Lett.* **85** 642
[7] Min C J, Wang P, Jiao X J, Deng Y and Ming H 2007 *Opt. Express* **15** 9541
[8] Ishii S, Kildishev A V, Shalaev V M, Chen K P and Drachev V P 2011 *Opt. Lett.* **36** 451
[9] Liu Y, Fu Y Q, Zhou X L, Xu Z W, Zeng G S and Fang F Z 2011 *Plasmonics* **6** 227
[10] Sriturayanich W, Pan L, Wang Y, Sun C, Bogy D B and Zhang X 2011 *Nat. Nanotech.* **3** 733
[11] Zheng G G and Li X Y 2009 *J. Opt. A: Pure Appl. Opt.* **11** 075002
[12] Lerman G M, Yanai Y and Levy U 2009 *Nano Lett.* **9** 2139
[13] Zhang Y, Zhao Q, Liao Z M and Yu D P 2009 *Chin. Phys. B* **18** 4865
[14] Zhu S and Wu J 2011 *Chin. Phys. B* **20** 067901
[15] Zhao Y H, Lin S C S, Nawaz A A, Kiraly B, Hao Q Z, Liu Y J and Huang T J 2010 *Opt. Express* **18** 23458
[16] Yu Y T and Zappe H 2011 *Opt. Express* **19** 9434
[17] Chen W, Abeysinghe D C, Nelson R L and Zhan Q W 2010 *Nano Lett.* **10** 2075
[18] Yang S, Chen W, Nelson R L and Zhan Q W 2009 *Opt. Lett.* **34** 3047
[19] Kim S, Kim H, Lim Y and Lee B 2007 *Appl. Phys. Lett.* **90** 051113
[20] Fan X and Wang G P 2006 *Opt. Lett.* **31** 1322
[21] Saj W M 2009 *Opt. Express* **17** 13615
[22] Gordon R 2009 *Phys. Rev. Lett.* **102** 207402
[23] Rance H J, Hamilton O K, Sambles J R and Hibbins A P 2009 *Appl. Phys. Lett.* **95** 041905
[24] Born M and Wolf E 2002 *Principles of Optics* (New York: Cambridge University Press)
[25] Johnson P B and Christy R W 1972 *Phys. Rev. B* **6** 4370
[26] Kim H, Park J and Lee B 2009 *Opt. Lett.* **34** 2569
[27] Kim S, Lim Y, Park J and Lee B 2010 *J. Lightwave Technol.* **28** 2023
[28] Søndergaard T, Bozhevolnyi S I, Novikov S M, Beermann J, Devaux E and Ebbesen T W 2010 *Nano Lett.* **10** 3123
[29] Lalanne P, Hugonin J P and Rodier J C 2005 *Phys. Rev. Lett.* **95** 263902
[30] Søndergaard T, Bozhevolnyi S I, Beermann J, Novikov S M, Devaux E and Ebbesen T W 2012 *J. Opt. Soc. Am. B* **29** 130
[31] Choi D, Lim Y, Roh S, Lee I M, Jung J and Lee B 2010 *Appl. Opt.* **49** A30
[32] Zhu Q F, Ye J S, Wang D Y, Gu B Y and Zhang Y 2011 *Opt. Express* **19** 9512
[33] Khoo E H, Li E P and Crozier K B 2011 *Opt. Lett.* **36** 2498
[34] S?ndergaard T, Bozhevolnyi S I, Novikov S M, Beermann J, Devaux E and Ebbesen T W 2010 *Nano Lett.* **10** 3123
[35] Stockman M I 2004 *Phys. Rev. Lett.* **93** 137404
[36] Fang Z Y, Qi H, Wang C and Zhu X 2010 *Plasmonics* **5** 207
[37] Xu T, Wu Y K, Luo X G and Guo L J 2010 *Nature Commun.* **1** 59
[38] Shi H F, Wang C T, Du C L, Luo X G, Dong X C and Gao H T 2005 *Opt. Express* **13** 6815
[39] Kim J K, Noemaun A N, Mont F W, Meyaard D, Schubert E F, Poxson D J, Kim H, Sone C and Park Y 2008 *Appl. Phys. Lett.* **93** 221111
[40] Smith D R, Mock J J, Starr A F and Schurig D 2005 *Phys. Rev. E* **71** 036609
[41] Mei Z L, Bai J and Cui T J 2010 *J. Phys. D: Appl. Phys.* **43** 055404
[42] Xu T, Wang C T, Du C L and Luo X G 2008 *Opt. Express* **16** 4753
[43] Bozhevolnyi S I, Volkov V S, Devaux E, Laluet J Y and Ebbesen T W 2006 *Nature* **440** 508
[44] Yang Y, Fu Y Q, Yao H M, Hu S, Zhou S L, Yan W, Chen W F, Cheng G X and Li Z 2009 *J. Comput. Theor. Nanos.* **5** 1030